# Modelling delamination of a DCB test using non-linear truss interface elements and plate elements with assumed shear strain

**I.Hlača*, D. Ribarić*, L. Škec* and M. R. Zefreh***

* Faculty of Civil Engineering
University of Rijeka
R. Matejčić 3, 51000 Rijeka, Croatia
e-mail: {ivan.hlaca, dragan.ribaric, leo.skec, maedeh.ranjbar}@gradri.uniri.hr

**Key words:** Fracture Mechanics, Delamination, Cohesive Zone Model, Finite Element Analysis.

**Abstract:** *In this work we are investigating mode I delamination of plate-like specimens, where the width is comparable to the length. In such cases anticlastic bending of the plates takes place on the debonded part and the crack front is a curve, rather than a straight line. We model the interface by means of discrete non-linear truss elements with embedded exponential traction-separation law. Such choice is justified because in this test, only pure mode I (opening) displacements occur at the interface, which in our case will cause axial elongation of the truss elements. The plates are modelled using 4-node plate finite elements derived by the assumed shear strain approach that pass the general constant-bending patch test. Cohesive-zone interface parameter identification is performed by a direct method (J-integral) and by virtual experiments regression. Numerical tests have been performed and the exponential cohesive-zone interface model compared against the bi-linear in terms of precision, robustness and computational time. The results confirm the experimentally observed behavior with anticlastic bending of the arms and the curved crack front.*

## 1 INTRODUCTION

Delamination is one of the most important and severe failure modes of composite structures. Resistance to delamination is essentially resistance to fracture of the interlayer connection, which is expressed in terms of fracture-mechanics parameters such as the critical energy release rate ($G_C$), the stress intensity factor ($K_C$) or the J integral.

Although in general there are three basic modes of delamination, as well as the combination of the basic modes (so-called mixed-mode delamination), in this work we will focus only on mode I (opening) delamination. Experimental studies of mode I delamination are commonly performed by so-called double cantilever beam (DCB) test [1,2]. For structural joints and composites, crack is introduced by inserting a thin film in otherwise glued interface and by pulling the specimen apart one is able to monitor the crack propagation.

Fracture mechanics is divided into discipline of linear elastic (LEFM) fracture mechanics and elastic-plastic fracture mechanics. In contrast to limit load analysis, fracture mechanics allows for modelling of inelastic behaviour and drop in load-carrying capabilities. Currently, this is usually done by using the so-called cohesive zone model (CZM) which was introduced by Dugdale and Barenblatt [3,4] in the early '60s of the last century. CZM is used in combination with finite element method by making the constitutive behaviour of material nonlinear. This nonlinearity requires iterative solver (e.g. Newton-Raphson method) and definition of so-called traction-separation law (TSL). By using the J-integral approach, one can experimentally determine the TSL from DCB experiment [5].

https://doi.org/10.4995/YIC2021.2021.12587

## 2 PROBLEM DESCRIPTION AND DCB TEST FOR PLATE-LIKE SPECIMEN

Double cantilever beam (DCB) test is the standard test for determining the fracture resistance in mode I. Typical geometry, boundary conditions and loading of the test is illustrated in Figure 1. Test specimens are made by gluing two equal adherends together in order to expose them to a symmetric opening load during the experiment, thus creating crack propagation along the bonded surface. Applied load, load-line displacement and crack length are continuously measured during the experiment. While the first two parameters can be obtained directly from the tensile-testing machine, for the measurement of the crack length, additional optical measuring equipment is required. The data obtained from the experiment is then used to compute the fracture toughness of the adhesive using methods known as data-reduction schemes [6]. Geometry and material properties used are given in Table 1.

**Table 1**: Geometry and material used.

| | |
|---|---|
| Aluminium layer | L = 250 mm |
| | B = 120 mm |
| | h = 6 mm |
| | $a_0$ = 45 mm |
| | E = 70 GPa |
| | $\nu$ = 0.33 |
| SikaPower®-4720 interface | t = 0.5 mm |
| | $G_{IC}$ = 1.15 N/mm$^2$ |
| | $\delta_0$ = 0.02 mm |
| | $\sigma$ = 21.15 MPa |

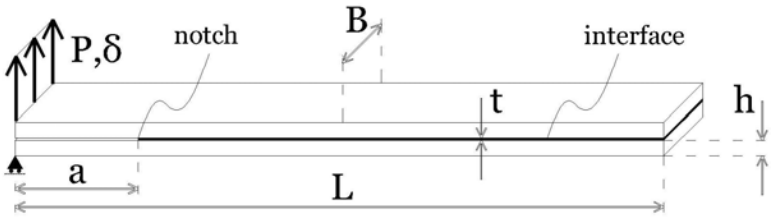


**Figure 1**: Geometry of a DCB specimen with corresponding boundary conditions and loading.

### 2.1 Critical energy release rate

Crack propagation occurs when G reaches critical value $G_C$. Furthermore, it was shown that this value equals,

$$G_C = \frac{P^2 dC}{2Bda} \tag{1}$$

By using the well-known beam theory expressions for cantilever beam deflection we can calculate the compliance and its derivative over change of the fractured area, i.e. we can derive the critical energy release rate $G_C$. Calculation of $G_C$ is usually done in accordance with international standards for determining the fracture resistance in mode I, namely ISO 25217:2009 and ASTM-D3433-99. Experimentally determined fracture resistance is used as a parameter in CZM model.

### 2.2 DCB test for plate-like specimen

To the best of authors' knowledge, there is no available method to determine fracture resistance of wide specimens where width is comparable to the length. In this scenario beam theory does not apply and crack front is not a straight line i.e. $dA \neq B \cdot da$ as defined in expression (2). Experimental findings show that the crack front is curved and that the crack length at the specimen's edges is shorter than at its center (see Figure 2). Earlier research [7] reported that curved crack front has a parabolic shape which is verified in this work.

International standards give instruction on how to measure the crack length along the edge of the specimen assuming that the crack front does not vary along the width of the specimen. However, this assumption becomes very questionable for relatively wide specimens. By using digital image correlation (DIC) it is possible to measure the crack without restricting it to the edges only. Measurement method takes advantage of the experiment symmetry.

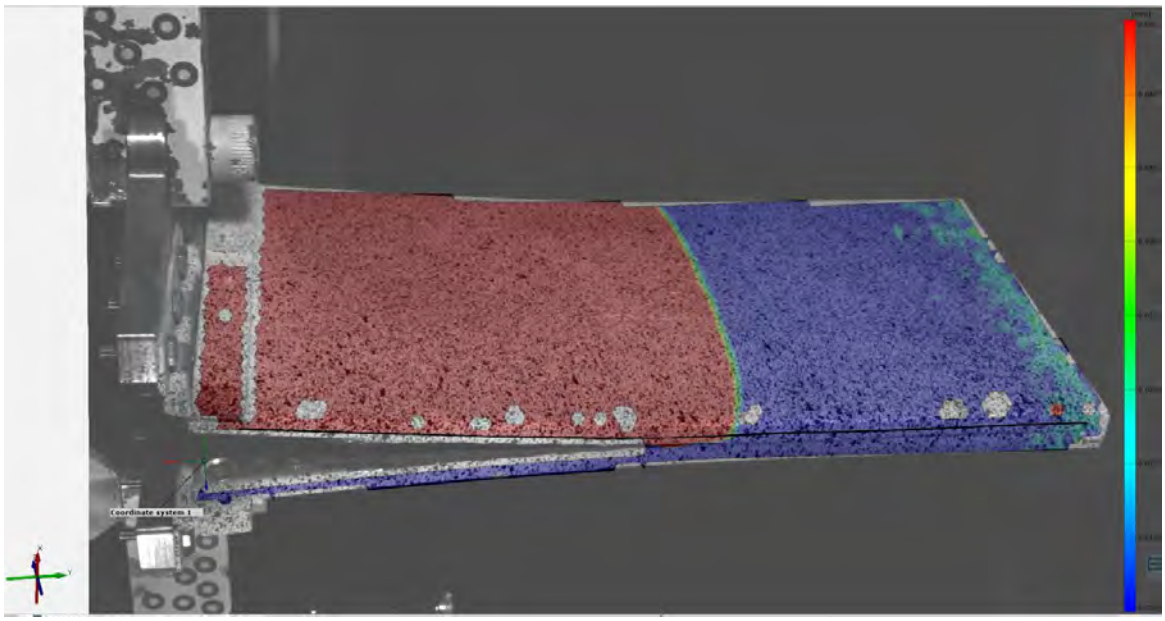

**Figure 2**: DCB test of wide specimens and observable crack front from the DIC measurement (debonded area is given in red).

## 3 MODELLING DELAMINATION

### 3.1 Cohesive zone model

In a cohesive zone model, a non-linear relationship with softening is introduced between the relative displacements at the interface and the corresponding tractions. Interface surfaces are able to lose cohesion and separate from one another as the interface traction $\sigma$ approach zero. At first, material behaves elastically, as it would in linear calculation, but after reaching the maximum traction, softening at the interface takes place.

### 3.2 Interface elements

Finite element analysis can use specific TSL for various interface elements, such as 1D spring or multi-node interface, e.g. INT-4, INT-8 [8]. Traction-separation laws can have various shapes, such as bi-linear, trapezoid, exponential, etc. This report will show the application of 1D truss/spring element with material described by exponential and bi-linear [9] TSL. Comparison between the two is shown on Figure 3. Exponential law used here is equivalent to Needleman's

mixed mode law [10] but for spring element application, where only mode I is sufficient, TSL is defined by the authors as follows,

$$\sigma\left(\delta\right) = \frac{G_C}{\delta_0^2}\delta \cdot e^{-\frac{\delta}{\delta_0}}, \tag{2}$$

$$K\left(\delta\right) = \frac{G_C}{\delta_0^2} \cdot e^{-\frac{\delta}{\delta_0}} \cdot \left(1 - \frac{\delta}{\delta_0}\right). \tag{3}$$

Area under the curve of TSL (Figure 3) is by definition equivalent to critical energy release rate $G_{IC}$. Other TSL parameters such as initial stiffness, maximum traction (maximum stress) and maximum elongation might be adopted from simple mechanical experiments but this is not practical nor reliable. Size effect and other influences result in different behavior for bulk material and cohesive material at interface.

Cohesive-zone interface parameter identification is performed by a direct method (J-integral) [5] and by virtual experiments regression. Exponential TSL parameters used here are retrieved from experiments on regular DCB tests [6] and they are mentioned earlier in Table 1. Bi-linear TSL law has two additional parameter $\delta_C$, $\sigma_{MAX}$ which can be reduced to either one of the two. Bi-linear TSL is chosen to match the maximum traction of exponential TSL by integrating Expression (2) and finding relation,

$$\sigma_{max} = G_C/(\delta_0 \cdot e) = 21.155\ MPa. \tag{4}$$

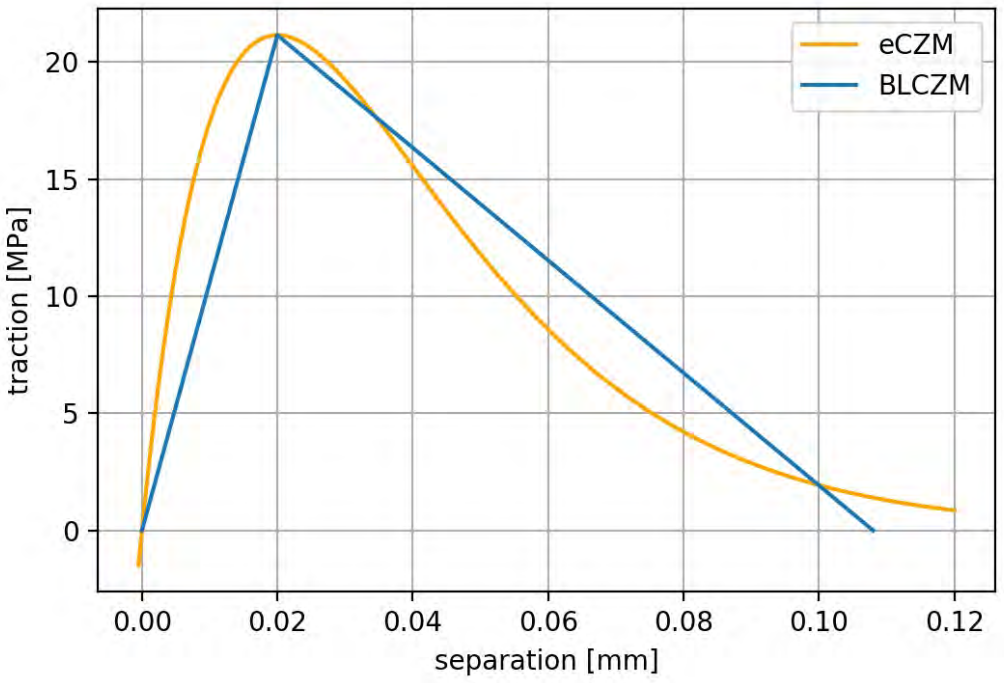


**Figure 3**: Exponential (eCZM) vs bi-linear (BLCZM) traction-separation law; critical energy release rate and maximum traction are both made equal for the two TSL.

### 3.3 Layer elements

Q4-U3 is a facet shell element desig ned for the general shell model analysis [11]. It is structured as a joined plate and in-plane (membrane) element whose stiffness matrices are

integrated for a 3D environment. The plate part is based on the cubic linked interpolations for lateral displacement and two section rotations, and since it is cubic it is also, problem dependent, e.g. the material parameters E, $\nu$ and thickness t are necessary values in the interpolations. The final expressions for strains (shear strains) are assumed in the simplified form, derived from the differential kinematic equations because they have to match the equilibrium equations too. The membrane part of interpolations is also displacement based and has the cubic form with higher order terms depending of the drilling nodal rotations similar to Allman's cubic interpolations for triangle membrane elements. Membrane part is not needed in delamination simulation considered in this work because in pure mode I delamination there are no in-plane (membrane) stresses.

### 3.4 Delamination model

The proposed numerical model makes use of truss interface elements with embedded exponential TSL and 4-node linked interpolation plate/shell element for the layers. Truss elements are perpendicular to the layers. Pre-processing and post-processing was done in Python while the main calculations were implemented in FEAP [12] where solution procedure minimizes the residual. At first, it checks the strain energy norm and then the residual norm before stopping. Equation (2) and (3) are implemented in a user material element along with the plate finite element from earlier chapter. Only one half of the DCB specimen is modelled due to the symmetry. Truss interface element has cross-sectional area equal to

$$A = \frac{(L - a_0) \cdot B}{(m-1) \cdot (n-1)}, \tag{5}$$

where $m, n$ are number of nodes across length and width respectively. Interface elements at edges have only half of the area $A$ from (5), while the four elements at vertices have the same area as if they were edge elements for simplicity only. Damage history variable that usually saves the value of maximum separation is not needed because no unloading or reloading occurs during a DCB experiment. One of the problems encountered was the inability to use a computationally lightweight mesh size while achieving a convergence in iterative residual minimization. Higher ductility of the interface parameters (higher $\delta_0$, $\delta_C$) and mesh refinements are the simplest way to improve convergence. It was found that type of finite element for layer also influences the result, especially the oscillations as reported in [8]. Advanced solution procedures, such as arc-length method [8], that can significantly improve convergence of delamination simulation, have not been used in this work. It has been found that the choice of interface TSL can have a strong influence on the convergence, which will be evident from the results in the next chapter.

## 4 COMPARISON OF RESULTS

### 4.1 Results

Minimum required finite element mesh for exponential TSL was found to be 50 x 10, which corresponds to element size of 5 x 12 mm. On the other hand, minimum required finite element mesh for bi-linear TSL was found to be 250 x 24 (or more), meaning that one finite element is as small as 1 x 5 mm. Mesh regularity (aspect ratio) could be improved for both cases but this would additionally increase the computational time, in particular for the bi-linear law, while not improving the results noticeably. Figure 4 and 5 show comparison with experimental force-displacement data on the left hand side graph. On the right hand side is the plot of layer separation where the yellow color represents delamination and the purple color represents portion that is still intact while the white color represents area of initial crack.

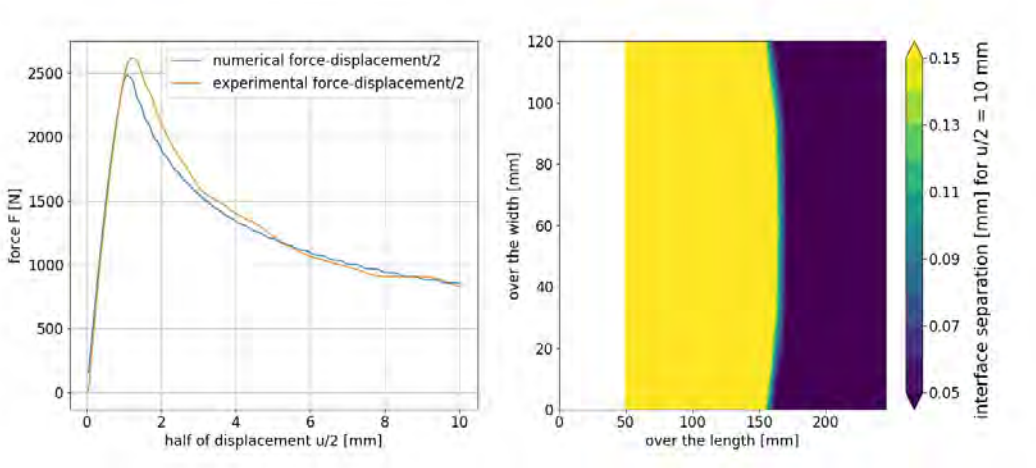


**Figure 4**: Results for exponential TSL

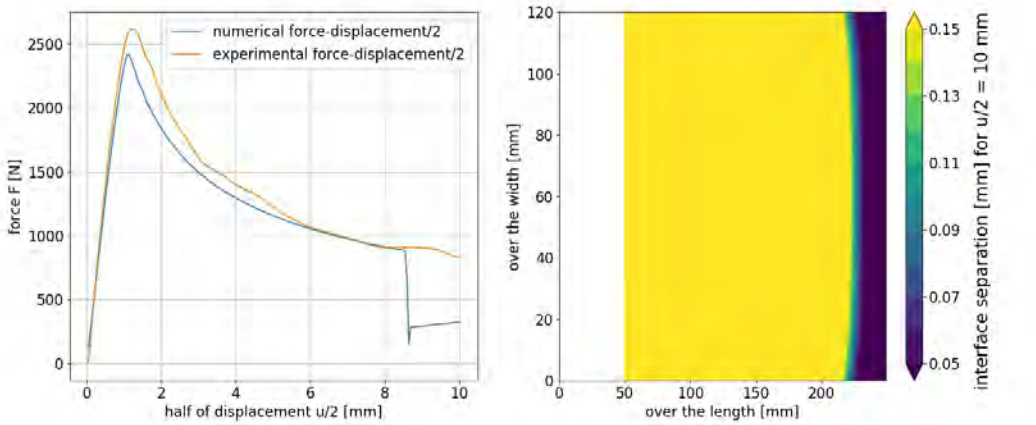


**Figure 5**: Results for bi-linear TSL

### 4.2 Performance assessment

In terms of robustness, we found that the exponential TSL, unlike the bi-linear TSL, is capable of converging even with oscillating behavior and large number of iterations. The model with the bi-linear TSL lost convergence near the end of virtual experiment (Figure 5) which suggests that minimum mesh size should in fact be even more refined, e.g. 250 x 48. Results for refined mesh are not presented here for the sake of brevity, but they approximately match the results in Figure 4 although with less oscillations due to increased number of FEM nodes (over 20 000).

Table 2 shows performance in terms of computational cost. It is found that exponential law again outperforms the bi-linear law. Our findings relate to a specific case with truss interface element and this may not translate to other scenarios because this was not observed earlier by other authors [8]. It is worth noting that the number of iterations per increment is approximately the same for different meshes used. Furthermore, exponential law as defined by (2) and (3) is continuous and does not need any IF statements in FEM code in contrast to bi-linear law which require a total of 3 IF statements. As shown in Table 2, the run-time needed to finish simulation is obviously in favor to the eCZM. Important factor that has substantial influence on convergence is the choice of finite element for the layers. All reported

observations were similar for FEAP's original SHELL element which actually showed better convergence properties in all cases. By taking into consideration shear strains of plate (or beam), delamination problems converge harder. Nevertheless, authors expect that the layer elements that account for shear deformation will show better behavior in scenarios with multi-node interface cohesive elements and solution procedures where mesh is sparser as this was the case in simpler benchmarks [11].

**Table 2**: Geometry and material used.

| | eCZM | BLCZM |
|---|---|---|
| Minimal mesh (No. of elements) | 50 x 10 | 250 x 24 |
| No. of nodes | 1012 | 11300 |
| Average No. of iterations per increment | 4.75 | 4.68 (before loss of convergence) |
| Run-time | 33 seconds | 47 minutes |

## 5 CONCLUSIONS

In this work, the curved crack front of a double cantilever beam specimen with width comparable to its length has been obtained experimentally and numerically. In addition, force vs displacement data for experimental and numerical results are in good agreement. Non-linear truss elements used to model delamination in conjunction with shell elements behave better in all aspects if exponential, rather than bi-linear, TSL is assumed. Benefits of elements with higher order interpolation were not noticed for relatively dense meshes used. On the contrary, accounting for shear strain introduced problems such as oscillations or even loss of convergence. Reasons behind this phenomenon will also be a topic of further study.

## REFERENCES

[1] British Standards Institution BS ISO 25217. (2009) Adhesives – Determination of the mode 1 adhesive joints using double cantilever beam and tapered double cantilever beam specimen. British Standard.

[2] ASTM D3433-99. (2012) Standard test method for fracture strength in cleavage of adhesives in bonded metal joints. ASTM International.

[3] Dugdale DS. Yielding of steel sheets containing slits. *JMech Phys Solids 1960*; **8**:100–4.

[4] Barenblatt GI. The mathematical theory of equilibrium cracks in brittle fracture. *Adv Appl Mech* 1962;**7**:55–129.

[5] Gorman, J. M. and Thouless, M. D. (2019) The use of digital-image correlation to investigate the cohesive zone in a double-cantilever beam, with comparisons to numerical and analytical models, *Journal of the Mechanics and Physics of Solids*, **123**, pp. 315–331. doi: 10.1016/j.jmps.2018.08.013.

[6] Hlača, I., Grbac, M. and Škec, L. (2019) Determining Fracture Resistance of Structural Adhesives in Mode-I Debonding Using Double Cantilever Beam Test, *Zbornik radova*, **22**(1), pp. 59–74. doi: 10.32762/zr.22.1.4.

[7] WIT Transactions on Engineering Sciences (1994). ISSN: 1743-3533, 251-258.

[8] Alfano, G. (2006) On the influence of the shape of the interface law on the application of cohesive-zone models, *Composites Science and Technology*, **66**(6), pp. 723–730. doi: 10.1016/j.compscitech.2004.12.024.

[9] Ranjbar, M., Jelenić, G., and Škec, L. (2020). Modelling Adhesive Using Non-Linear Truss Elements in Mode I Delamination Problems, *Zbornik radova*, XXIII(1), 29-40. https://doi.org/10.32762/zr.23.1.2

[10] Xu, X. P. and Needleman, A. (1993) Continuum Modelling of Interfacial Decohesion, *Solid State Phenomena*, 35–36, pp. 287–302. doi: 10.4028/www.scientific.net/ssp.35-36.287.

[11] Ribarić, D. (2016) Problem-dependent cubic linked interpolation for Mindlin plate four-node quadrilateral finite elements, *Structural Engineering and Mechanics*, **59**(6), pp. 1071–1094. doi: 10.12989/sem.2016.59.6.1071.

[12] Taylor, R.L. FEAP - Finite Element Analysis Program Published: 2014 Publisher: University of California, Berkeley URL: http://www.ce.berkeley/feap